EFFECT OF THERMAL RADIATION AND CHEMICAL REACTION ON UNSTEADY MHD FREE CONVECTION FLOW OF AN INCOMPRESSIBLE FLUID PAST AN INFINITE VERTICAL POROUS PLATE IN PRESENCE OF VISCOUS DISSIPATION

M. Anil Kumar[1] Y. Dharmendar Reddy[2] V. Srinivasa Rao[3]

[1,2,3]Department of Mathematics, Anurag Group of Institutions, Venkatapur, Ghatkesar, Medchal , Telangana

Author Email id's: dharmayanala@gmail.com[1], anilradhi2010@gmail.com[2] and uhita@yahoo.com[3]

ABSTRACT

In this paper a numerical investigate made on the Heat and mass transfer effects on an unsteady MHD free convective flow of a chemically reacting incompressible fluid over an infinite vertical porous plate through a porous medium in the presence of viscous dissipation and thermal radiation. The governing system of equations is solved using Galerkin finite element method. Velocity, temperature and concentration fields are discussed graphically. Also the effects of skin friction coefficient, Nusselt number and Sherwood number are presented numerically in a tabular form. The results are in good agreement with the earlier studies.

Keywords: MHD, porous medium, Viscous Dissipation, Finite element method, Thermal Radiation

List of variables:

C'_∞	Concentration of the fluid far away from the plate ($Kg\ m^{-3}$)
C'_w	Concentration of the plate ($Kg\ m^{-3}$)
y	Dimensionless displacement (m)
T'_∞	Fluid temperature away from the plate (K)
Gm	Grashof number for mass transfer
Gr	Grashof number for heat transfer
u	Non-dimensional fluid velocity ($m\ s^{-1}$)
Sh	The local Sherwood number
u'	Velocity component in $x'-$ direction ($m\ s^{-1}$)
g	Acceleration of gravity, 9.81 ($m\ s^{-2}$)
x'	Coordinate axis along the plate (m)
y'	Co-ordinate axis normal to the plate (m)
Ec	Eckert number
C'	Fluid Concentration ($Kg\ m^{-3}$)
T'	Fluid Temperature (K)
T'_w	Fluid temperature at the wall (K)
M	Magnetic parameter
Pr	Prandtl number
q_r	Radiative heat transfer coefficient
Re	Reynolds number
Sc	Schmidt number
D	Solute mass diffusivity ($m^2\ s^{-1}$)
C_p	Specific heat at constant pressure $\left(J\ Kg^{-1}K\right)$
Nu	The local Nusselt number

τ Skin Friction

B_0 Uniform magnetic field (*Tesla*)

H_O Magnetic Induction

K_r chemical reaction

Greek Symbols:

κ Thermal conductivity of the fluid ($W\ m^{-1}K^{-1}$)

θ Non dimensional fluid temperature (K)

β^* Volumetric Coefficient of thermal expansion with concentration ($m^3\ Kg^{-1}$)

σ Electric conductivity of the fluid ($s\ m^{-1}$)

ν Kinematic viscosity ($m^2\ s^{-1}$)

μ_o Magnetic Permeability ($N.A^{-2}$)

C Species concentration ($Kg\ m^{-3}$)

ρ The constant density ($Kg\ m^{-3}$)

β Volumetric coefficient of thermal expansion (K^{-1})

Superscripts:

' Dimensionless Properties

Subscripts:

∞ Free stream conditions

p Plate

w Conditions on the wall

INTRODUCTION

Modern applications of heat and mass transfer plays vital role in engineering and science applications such as energy systems, thermal energy storage, high capacity active cooling systems, controlled rate of combustion, fuel cells. The advantages of the latent heat thermal energy systems are a large amount of heat can be absorbed and released at a constant temperature. The size of the latent heat thermal energy system is considerably smaller than its counterpart using sensible heat thermal storage. A fuel cell is an electro chemical energy device that converts the chemical energy in the fuel directly into electrical energy. It is becoming increasingly attractive alternatives to other conversion technologies, from small-scale passive devices like batteries to large scale thermodynamic cycle engines. Combustion is a chemical reaction process between a fuel and an oxidant that produces high-temperature gases. Due to its applications many researchers have studied and doing their research on MHD free convective flow in a porous medium. Hossain and Mandal [1] investigated mass transfer effects on unsteady hydromagnetic free convective flow past an accelerated vertical plate. Michalis Xenos et al [2] studied the effect of constant uniform suction on unsteady MHD free convection flow of water at 4˚C past an infinitely vertical moving plate with constant velocity. Mass transfer effects on an unsteady MHD free convective flow of an incompressible viscous dissipative fluid past an infinite vertical porous plate was studied by Prabhakar Reddy [3]. Siva Reddy Sheri and Srinivasa Raju [4] demonstrated the effect of thermal diffusion (Soret) on unsteady hydrodynamic free convection flow past a semi-infinite vertical plate in the presence viscous dissipation.

Radiation plays vital role in heating and cooling chambers, fossil fuel combustion, energy process & astrophysical flows. The effect of thermal radiation on flow and heat transfer processes is of major importance in the design of many advanced energy conversion systems operating at high temperature. Pandya and Shukla [5] investigated Soret - Dufour and radiation effects on unsteady MHD flow past an impulsively started inclined porous plate with variable temperature and mass diffusion. Hussanan et al. [6] investigated the influence of heat transfer on the unsteady boundary layer flow of a Casson fluid past an infinite oscillating vertical plate in presence of Newtonian heating using Laplace transform method. Olarewaju [7] studied similarity solution for natural convection from a moving vertical plate with internal heat generation and a convective boundary condition in the presence of thermal radiation and viscous dissipation. Attia and Ahmed [8] considered the Couette flow and heat transfer between parallel plates in an electrically conducting Casson fluid.

Venkateswarlu et al. [9] examined the effects of chemical reaction and heat generation on MHD boundary layer flow of a moving vertical plate with suction and dissipation. Sarada and Shanker [10] studied the effects of Soret and Dufour on an unsteady MHD free convection flow past a vertical porous plate in the presence of suction or injection. N. Vedavathi et al. [11] analyzed the Radiation and mass transfer effects on unsteady MHD convective flow past an infinite vertical plate with Dufour and Soret effects. Ming-chun et al. [12] took an account of the thermal diffusion and diffusion-thermo effects, to study the properties of the heat and mass transfer in a strongly endothermic chemical reaction system for a porous medium. Effect of radiation and soret in the presence of heat source/sink on unsteady MHD flow past a semi-infinite vertical plate was studied by Srihari and Srinivas [13]. D. Srinivasacharya and Ch. RamReddy [14] studied the Soret and Dufour effects on mixed convection from an exponentially stretching surface. Rashidi et al. [15] delved into the studied of heat transfer of a steady incompressible water base nanofluid flow over a stretching sheet in the presence of transverse magnetic field with thermal radiation and buoyancy effects. Srinivasa Rao et al. [16] examined Soret and Dufour effects on MHD boundary layer flow over a moving vertical porous plate with suction. Mohammed Ibrahim[17] investigated an unsteady MHD convective heat and mass transfer past an infinite vertical plate embedded in a porous medium with radiation and chemical reaction under the influence of Dufour and Soret effects. R. Srinivasa Raju et. al [18] discussed the Analytical and Numerical study of unsteady MHD free convection flow over an exponentially moving vertical plate with Heat Absorption. Yih [19] numerically analyzed the effect of transportation velocity on the heat and mass transfer characteristics of mixed convection about a permeable vertical plate embedded in a saturated porous medium under the coupled effects of thermal and mass diffusion.

The objective of the present paper is to study the effects of thermal radiation and chemical reaction on MHD Free convective flow of an incompressible fluid past a vertical plate in the presence of viscous dissipation. The non dimensional governing coupled partial differential equations are involved in the present analysis and are solved by finite element Galerkin method which is more economical from computational point of view.

FORMULATION OF THE PROBLEM

Consider an unsteady free convective flow of an incompressible electrically conducting viscous dissipative fluid past an infinite vertical plate. The physical coordinate of the problem is as shown in the Figure A. Let x'-axis be chosen along the plate in the vertically upward direction and the y'-axis is chosen normal to the plate. A uniform Magnetic field of intensity H_0 is applied transversely to the plate. The induced magnetic field is neglected as the magnetic Reynolds number of the flow is taken to be very small. Initially, the temperature of the plate and fluid are T' and $T_\infty{}'$ are assumed to be the same. The concentration of species at the plate $C_w{}'$ and in the fluid throughout $C_\infty{}'$ is assumed to be the same. At time t'>0 the plate temperature is changed to $T_w{}'$, which is then maintained constant, causing convection currents to flow near the plate and mass is supplied at a constant rate to the plate.

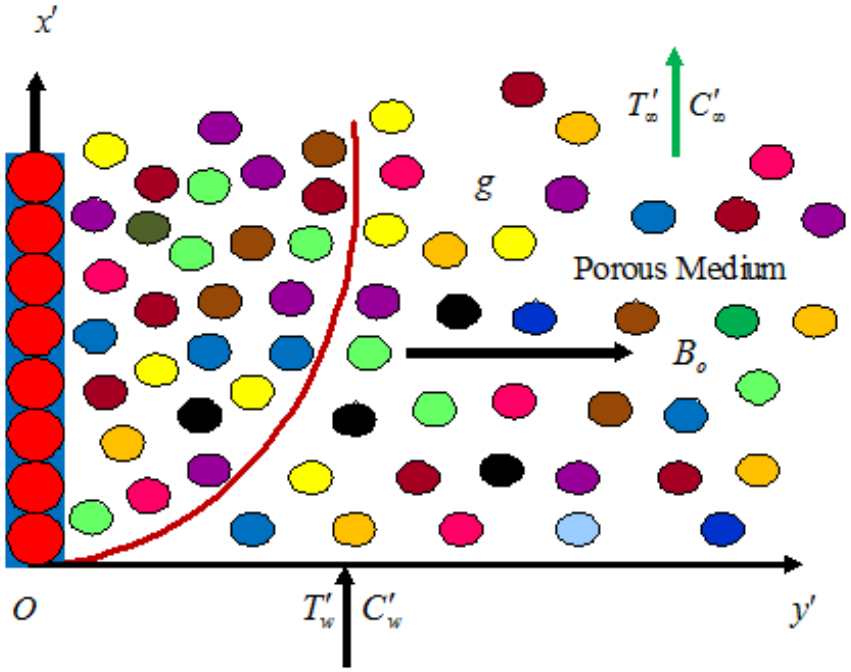

Figure A. Physical sketch and geometry of the problem

Under these conditions the flow variables are functions of time y' and t' alone. Under the usual Boussinesq approximation, the problem is governed by the following equations.

$$\frac{\partial v'}{\partial y'} = 0 \tag{1}$$

$$\frac{\partial u'}{\partial t'} = v\frac{\partial^2 u}{\partial y'^2} + g\beta(T' - T_\infty{}') + g\beta^*(C' - C_\infty{}') - \frac{\sigma\mu_e{}^2 H_0{}^2 u'}{\rho} - \frac{vu'}{K'} \tag{2}$$

$$\rho C_p \frac{\partial T'}{\partial t'} = k\frac{\partial^2 T'}{\partial y'^2} - \frac{\partial q_r}{\partial y'} + \mu(\frac{\partial u'}{\partial y'})^2 \tag{3}$$

$$\frac{\partial C'}{\partial t'} = D_M \frac{\partial^2 C'}{\partial y'^2} - Kr'(C' - C'_\infty) \tag{4}$$

The boundary conditions for the velocity, temperature and concentration fields are:

$$t' \le 0, u' = 0, T' = T_\infty{}', C' = C_\infty{}' \forall y'$$

$$u' = 0,\ T' = T'_w,\ \ C' = C'_w \text{ at } \quad y' = 0$$

$$u' \to 0, T' \to T'_\infty, C' \to C'_\infty \quad \text{as} \quad y' \to \infty \tag{5}$$

Where T'_w and C'_w are the wall dimensional temperature and concentration respectively.

Equation (1) gives $v' = -v_0 (v_o > 0)$

Where v_0 is the constant suction velocity & negative sign is indicates that it is towards the plate.

The radiative heat flux term by using Roseland approximation is given by

$$q_r = -\frac{4\sigma}{3k_1}\frac{\partial T'^4}{\partial y'} \tag{6}$$

Where k_1 and σ are mean absorption coefficient and Stefan Boltzmann constant respectively. It is assumed that the temperature difference within the flow are sufficiently small such that T'^4 May be expressed as a linear function of the temperature this is accomplished by expanding in a Taylor series about T'_∞ and neglecting the higher order terms, thus

$$T'^4 \cong 4T'^3_\infty T' - 3T'^4_\infty \tag{7}$$

Then Using (5) and (6) in equation (2), is reduced

$$\rho C_p \frac{\partial T'}{\partial t'} = k\frac{\partial^2 T'}{\partial y'^2} + \frac{16\sigma T'^3_\infty}{3k_1}\frac{\partial^2 T'}{\partial y'^2} + \mu\left(\frac{\partial u'}{\partial y'}\right)^2 \tag{8}$$

In order to write the governing equations and boundary condition in dimension less form the following non dimensional quantities are introduced.

$$M = \frac{\sigma\mu_0^2 H_0^2 \nu}{\rho v_o^2},\ u = \frac{u'}{u_o}, y = \frac{y' v_0}{\nu},\ t = \frac{t' v_o^2}{\nu},\ \theta = \frac{T' - T'_\infty}{T'_w - T'_\infty},\ C = \frac{C' - C'_\infty}{C'_w - C'_\infty},\ K = \frac{K' v_o^2}{\nu^2},\ \Pr = \frac{\mu c_p}{k},$$

$$Gm = \frac{g\beta^*(C'_w - C'_\infty)\nu}{u_o v_o^2},\ Kr = \frac{Kr'\nu}{v_o^2},\ Sc = \frac{\nu}{D_M}, Ec = \frac{u_0^2}{C_p(T'_w - T'_\infty)},\ R = \frac{4\sigma T'^3_\infty}{kk_1}, Gr = \frac{\nu g\beta(T'_w - T'_\infty)}{u_o v_o^2}$$

$$C_f = \frac{\tau'\omega}{\rho U_o \nu} = \left(\frac{\partial u}{\partial y}\right)_{y=0} \tag{9}$$

In view of (8), the equations (1), (3), (7) reduced to the following dimensionless form

$$\frac{\partial u}{\partial t} = Gr\theta + GmC + \frac{\partial^2 u}{\partial y^2} - (M + \frac{1}{K})u \tag{10}$$

$$\frac{\partial \theta}{\partial t} = \frac{1}{\Pr}(1 + \frac{4R}{3})\frac{\partial^2 \theta}{\partial y^2} + Ec(\frac{\partial u}{\partial y})^2 \tag{11}$$

$$\frac{\partial C}{\partial t} = \frac{1}{Sc}\frac{\partial^2 C}{\partial y^2} - KrC \tag{12}$$

And these corresponding boundary conditions are

$$\begin{aligned} &t \le 0 : u = 0, \theta = 0, C = 0\ \forall y, \\ &t > 0 : u = 0, \theta = 1, C = 1\ at\ y = 0 \\ &u \to 0, T \to 0, C \to 0\ as\ y \to 0 \end{aligned} \tag{13}$$

METHOD OF SOLUTION

Finite element technique is used to solving the non-dimensional momentum and energy equations (10) (11) and (12) along with the imposed boundary conditions (13).

The Galerkin expression for the differential equation (9) becomes

$$\int_{y_j}^{y_k} \left\{ N^T \left[\frac{\partial^2 u^{(e)}}{\partial y^2} - \frac{\partial u^{(e)}}{\partial t} - R u^{(e)} + P \right] \right\} dy = 0$$

Where $N^T = \begin{bmatrix} N_j & N_k \end{bmatrix}^T = \begin{bmatrix} N_j \\ N_k \end{bmatrix}$, $R = M + \frac{1}{K}$, $P\,(=Gr)T + (G_m)C$;

Let the linear piecewise approximation solution

$$u^{(e)} = N_j(y)u_j(t) + N_k(y)u_k(t) = N_j u_j + N_k u_k$$

The element equation is given by

$$\int_{y_j}^{y_k} \left\{ \begin{bmatrix} N_j^{'} N_j^{'} & N_j^{'} N_k^{'} \\ N_j^{'} N_k^{'} & N_k^{'} N_k^{'} \end{bmatrix} \begin{bmatrix} u_j \\ u_k \end{bmatrix} \right\} dy + \int_{y_j}^{y_k} \left\{ \begin{bmatrix} N_j N_j & N_j N_k \\ N_j N_k & N_k N_k \end{bmatrix} \begin{bmatrix} \dot{u}_j \\ \dot{u}_k \end{bmatrix} \right\} dy + \mathrm{R} \int_{y_j}^{y_k} \left\{ \begin{bmatrix} N_j N_j & N_j N_k \\ N_j N_k & N_k N_k \end{bmatrix} \begin{bmatrix} u_j \\ u_k \end{bmatrix} \right\} dy$$

$$= \mathrm{P} \int_{y_j}^{y_k} \begin{bmatrix} N_j \\ N_k \end{bmatrix} dy$$

Where prime and dot denotes differentiation w.r.to ‘y’ and‘t’ respectively

Simplifying we get

$$\frac{1}{l^{(e)^2}} \begin{bmatrix} 1 & -1 \\ -1 & 1 \end{bmatrix} \begin{bmatrix} u_j \\ u_k \end{bmatrix} + \frac{1}{6} \begin{bmatrix} 2 & 1 \\ 1 & 2 \end{bmatrix} \begin{bmatrix} \dot{u}_j \\ \dot{u}_k \end{bmatrix} + \frac{R}{6} \begin{bmatrix} 2 & 1 \\ 1 & 2 \end{bmatrix} \begin{bmatrix} u_j \\ u_k \end{bmatrix} = \frac{P}{2} \begin{bmatrix} 1 \\ 1 \end{bmatrix}$$

Where $l^{(e)} = y_k - y_j = h$

In order to get the differential equation at the knot x_i, we write the element equations for the elements $y_{i-1} \le y \le y_i$ and $y_i \le y \le y_{i+1}$ assemble two element equations, we obtain

$$\frac{1}{l^{(e)^2}} \begin{bmatrix} 1 & -1 & 0 \\ -1 & 2 & -1 \\ 0 & -1 & 1 \end{bmatrix} \begin{bmatrix} u_{i-1} \\ u_i \\ u_{i+1} \end{bmatrix} + \frac{1}{6} \begin{bmatrix} 2 & 1 & 0 \\ 1 & 4 & 1 \\ 0 & 1 & 2 \end{bmatrix} \begin{bmatrix} \dot{u}_{i-1} \\ \dot{u}_i \\ \dot{u}_{i+1} \end{bmatrix} + \frac{R}{6} \begin{bmatrix} 2 & 1 & 0 \\ 1 & 4 & 1 \\ 0 & 1 & 2 \end{bmatrix} \begin{bmatrix} u_{i-1} \\ u_i \\ u_{i+1} \end{bmatrix} = \frac{P}{2} \begin{bmatrix} 1 \\ 2 \\ 1 \end{bmatrix}$$

We put the row equation corresponding to the knot ‘i’, is

$$\frac{1}{l^{(e)^2}} \left[-u_{i-1} + 2u_i - u_{i+1} \right] + \frac{1}{6} \left[\dot{u}_{i-1} + 4\dot{u}_i + \dot{u}_{i+1} \right] + \frac{R}{6} \left[u_{i-1} + 4u_i + u_{i+1} \right] = P$$

Applying Crank-Nicholson method to the above equation then we get

$$A_1 u_{i-1}^{n+1} + A_2 u_i^{n+1} + A_3 u_{i+1}^{n+1} = A_4 u_{i-1}^{n} + A_5 u_i^{n} + A_6 u_{i+1}^{n} + 24Pk$$

Where $A_1 = 2 + (R*k) - (6*r)$; $A_2 = (4*R*k) + (12*r) + 8$; $A_3 = 2 + (R*k) - (6*r)$;

$A_4 = 2 - (R*k) + (6*r)$; $A_5 = 8 - (4*R*k) - (12*r)$; $A_6 = 2 - (R*k) + (6*r)$; (14)

Applying similar procedure to equation (10), we get

$$B_1 T_{i-1}^{n+1} + B_2 T_i^{n+1} + B_3 T_{i+1}^{n+1} = B_4 T_{i-1}^{n} + B_5 T_i^{n} + B_6 T_{i+1}^{n}$$

B1= (2*Pr) - (6*r); B2= (8*Pr) + (12*r); B3= (2*Pr) - (6*r);

B4= (2*Pr) + (6*r); B5= (8*Pr) - (12*r); B6= (2*Pr)+(6*r); (15)

Applying similar procedure to equation (11), we get

$$J_1 C_{i-1}^{n+1} + J_2 C_i^{n+1} + J_3 C_{i+1}^{n+1} = J_4 C_{i-1}^{n} + J_5 C_i^{n} + J_6 C_{i+1}^{n}$$

J1= (2*Sc) -(6*r)+(Kr*Sc*k); J2= (8*Sc) + (12r)+ (4*Kr*Sc*k); J3=(2*Sc)-(6*r)+(Kr*Sc*k)

J4= (2*Sc) + (6*r)- (Kr*Sc*k); J5= (8*Sc) - (12r)- (4*Kr*Sc*k); J6=(2*Sc)+(6*r)-(Kr*Sc*k)

(16)

Where, Here r = $\frac{k}{h^2}$ and k, h are mesh sizes along y- direction and time-direction respectively index 'i' refers to space and 'j' refers to time .The mesh system consists of h = 0.1 and k = 0.001.

In the equations (11), (12), and (13), taking i = 1(1)n and using boundary conditions (10), then we get the following system of equations are obtained:

$$A_i X_i = B_i \quad \text{for} \quad i=1(1)n$$

Where A_i's are matrices of order n and X_i, B_i's are column matrices having n-components. The solutions of above system of equations are obtained by using Thomas Algorithm for velocity, temperature and concentration. Also, numerical solutions for these equations are obtained by C++ program. In order to prove the convergence and stability of Galerkin finite element method, the same C++ program was run with smaller values of h and k, no significant change was observed in the values of u, T and C. Hence the Galerkin finite element method is stable and convergent.

Table 1: The numerical values of *u*, *θ* and *C* for variation of mesh sizes

Mesh (Grid) size = 0.01			Mesh (Grid) size = 0.001			Mesh (Grid) size =0.0001		
U	*θ*	*C*	*U*	*θ*	*C*	*u*	*θ*	*C*
0.0000000	1.0000000	1.0000000	0.0000000	1.0000000	1.0000000	0.0000000	.0000000	1.0000000
0.1591205	0.5267089	0.4055494	0.1591204	0.5267089	0.4055494	0.1591205	0.5267088	0.4055494
0.1310582	0.2104376	0.1508049	0.1310581	0.2104376	0.1508049	0.1310582	0.2104375	0.1508049
0.0845936	0.0630920	0.495627	0.0845936	0.0630920	0.495627	0.0845935	0.0630920	0.495627
0.0495707	0.0142021	0.140290	0.0495707	0.0142021	0.140290	0.0495707	0.0142021	0.140290
0.0272283	0.0003139	0.0033705	0.0272282	0.0003139	0.0033705	0.0272283	0.0003139	0.0033705
0.0141074	0.0000025	0.0006831	0.0141074	0.0000025	0.0006831	0.0141074	0.0000025	0.0006831
0.001732	0.0000002	0.000169	0.001732	0.0000002	0.000169	0.001731	0.0000002	0.000169
0.0000000	0.0000000	0.0000000	0.0000000	0.0000000	0.0000000	0.0000000	0.0000000	0.0000000

Study of Grid independence

In general, to study the grid independency/dependency, the mesh size should be varied in order to check the solution at different mesh (grid) sizes and get a range at which there is no variation in the solution. The numerical values of velocity, temperature and concentration for different values of mesh (grid) size at 0.01, 0.001, and 0.0001 are shown in the following Table 1. From this table, we observed that there is no variation in the values of velocity, temperature and concentration for different values of mesh (grid) size at time. Hence, we conclude that, the results are independent of mesh (grid) size.

RESULTS AND DISCUSSION

The problem of thermal radiation and chemical reaction on MHD free convective flow of an incompressible fluid past a vertical plate in the presence of viscous dissipation is addressed in this study. Numerical calculations have been carried out for the non-dimensional velocity *(u)*, Temperature *(θ)*, and Concentration *(C)*. The numerical calculations of these results are presented graphically in Figures 1 to 13.

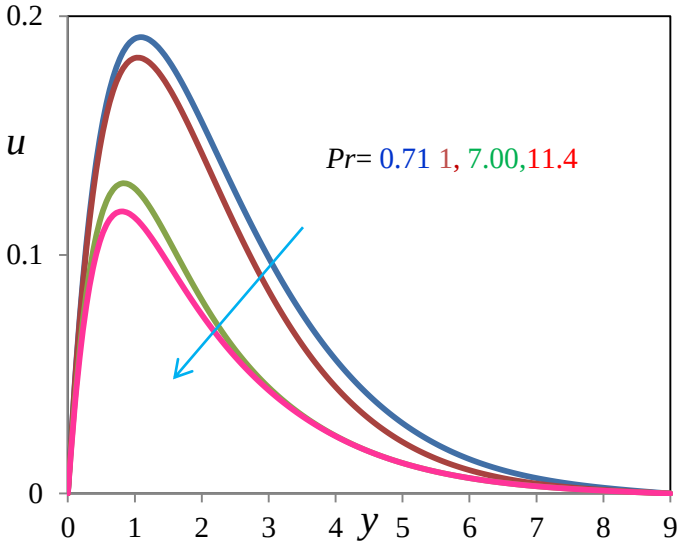

Figure 1. Velocity Profile for different values of *Pr* when *K=0.5, M=0.5, Ec=0.1, Sc=0.22, Gm=0.5, Gr=0.5, Kr=1.0, R=1.0*

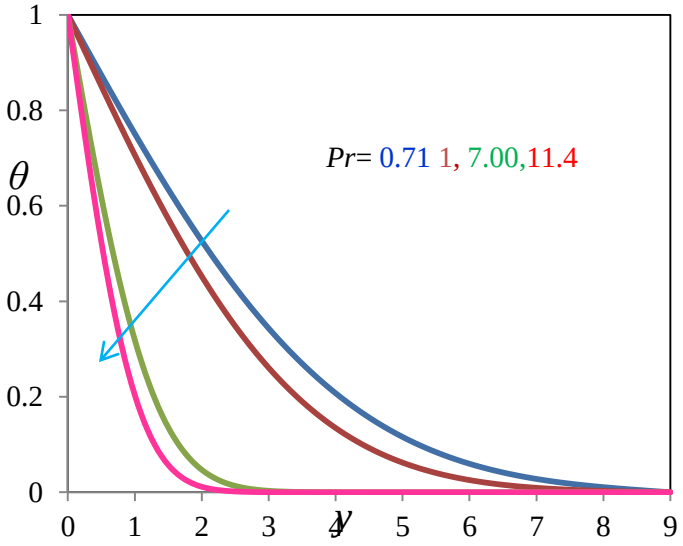

Figure 2. Temperature Profile for different values of *Pr* when *K=0.5, M=0.5, Ec=0.1, Sc=0.22, Gm=0.5, Gr=0.5, Kr=1.0, R=1.0*

The effect of prandtl number on the velocity and temperature profiles is shown in Figures 1 and 2 Prandtl number defined as the ration of kinematic viscosity to mass diffusivity. It is observed that the velocity profile decreases with the increase in Prandtl number *Pr*; this is due to the fact that fluids with higher Prandtl number possess greater viscosities and

this will serve to reduce velocities, thereby lowering the skin friction. In the same vein, an increase in the Prandtl number corresponds to a decrease in the temperature and the thermal boundary layer thickness. This is because for small values of the Prandtl number *Pr*(<1), the fluid is highly conductive.

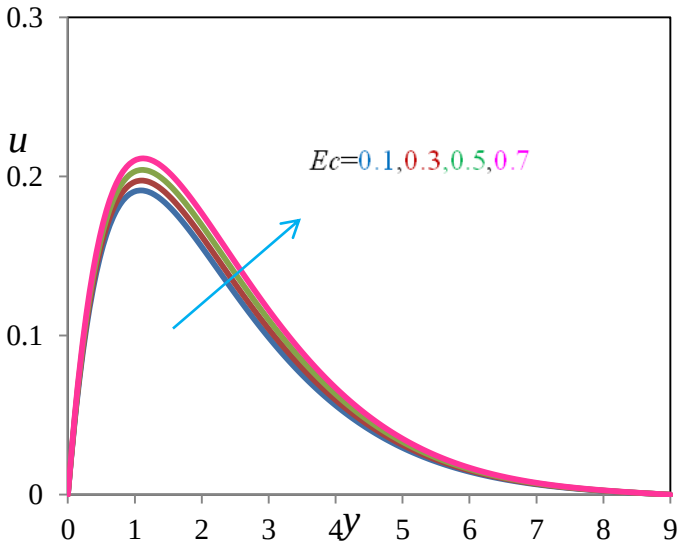

Figure 3. Velocity Profile for different values of *Ec* when *K=0.5, M=0.5, Pr=0.71, Sc=0.22, Gm=0.5, Gr=0.5, Kr=1.0 , R=1.0*

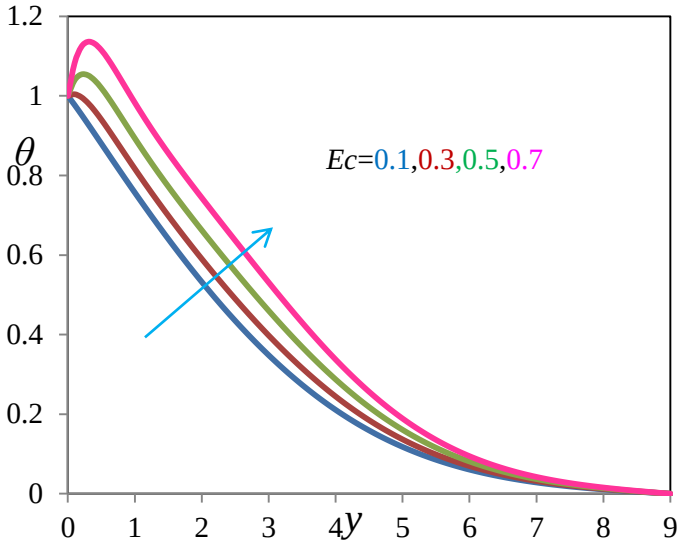

Figure 4. Temperature Profile for different values of *Ec* when *K=0.5, M=0.5, Pr=0.71, Sc=0.22, Gm=0.5, R=1.0, Gr=0.5,Kr=1.0*

Figures 3 and 4 illustrate the velocity and temperature profiles for different values of *Ec*. The Eckert number, *Ec*, expresses the relationship between the kinetic energy in the flow and enthalpy. It embodies the conversion of Kinetic energy into internal energy by work done against the viscous fluid stresses, and this energy is dissipated as heat. Greater viscous dissipative heat therefore causes a rise in temperature as well as the velocity.

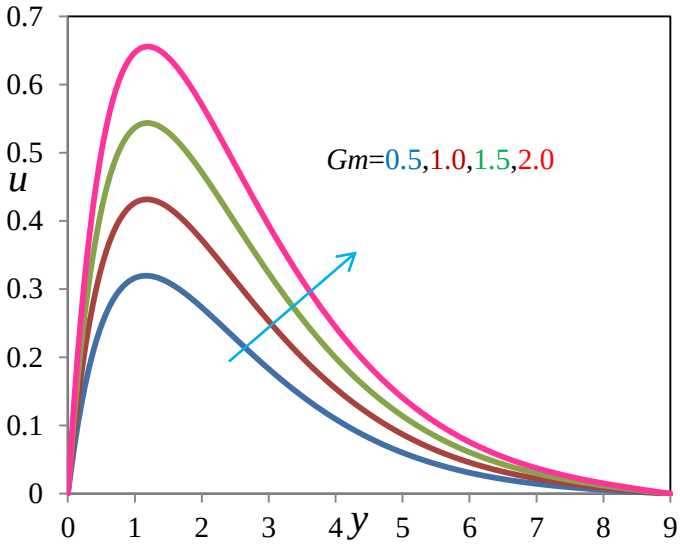

Figure 5. Velocity Profile for different values of *Gm* when *K=0.5, M=0.5, Ec=0.1, Sc=0.22, Pr=0.71, R=1.0, Gr=0.5,Kr=1.0*

From figure 5 it can be clearly seen that the velocity will increase with the increase in *Gm*. Modified Grashof number approximates the ratio of the concentration buoyancy force to viscous force acting on a fluid, increasing of *Gm* leads to increasing in the buoyancy force as well as decreasing the viscous forces. When viscosity decrease then internal resistance of the fluid will decrease, so automatically the fluid velocity will increase.

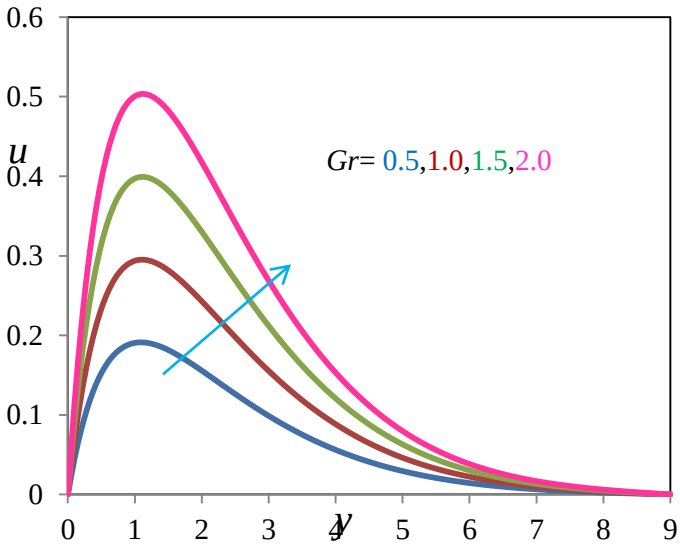

Figure 6. Velocity Profile for different values of *Gr* when *Pr=0.71, M=0.5, Ec=0.1, Sc=0.22, Gm=0.5, R=1.0,K=0.5, Kr=1.0*

Grashof number approximates the ratio of the buoyancy to viscous force acting on a fluid, increasing of Gr leads to increasing in the buoyancy force as well as decreasing the viscous forces. When viscosity decrease then internal resistance of the fluid will decrease, so automatically the fluid velocity will increase.

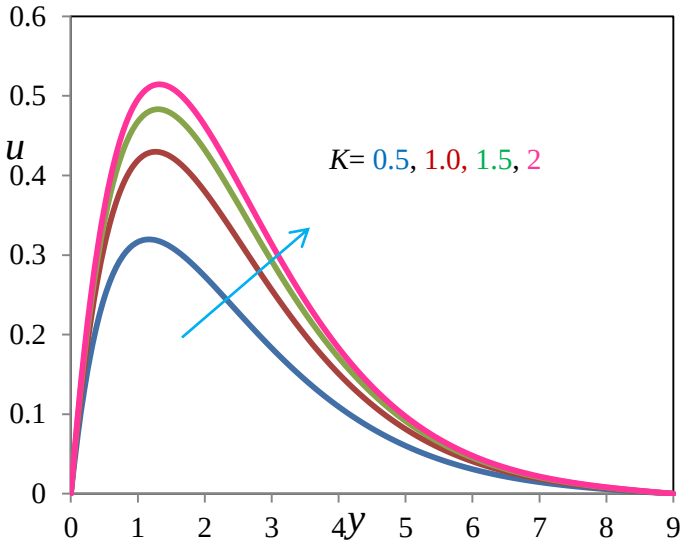

Figure 7. Velocity Profile for different values of *K* when *Pr=0.71, M=0.5, Ec=0.1, Sc=0.22, Gm=0.5, R=1.0, Gr=0.5, Kr=1.0*

Figure 7 illustrate the velocity profile for different values of porosity parameter *K*. Permeability are an important parameter for characterizing the transport properties that is heat and mass transfer in porous medium. It is observed that as *K* increases the velocity increases, because increase in permeability of medium implies less resistance due to the porous matrix present in the medium.

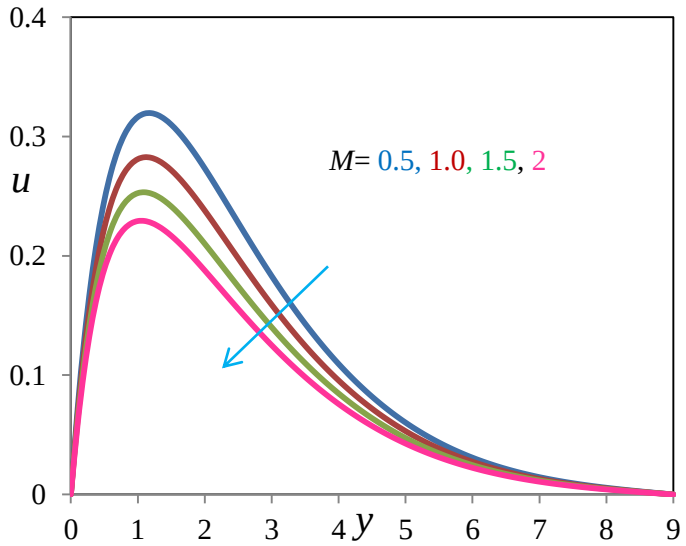

Figure 8. Velocity Profile for different values of *M* when *K=0.5, Pr=0.71, Ec=0.1, Sc=0.22, Gm=0.5, R=1.0, Gr=0.5, Kr=1.0*

Figure 8 has been plotted to depict the variation of velocity profile against Magnetic field parameter *M*. It is found that an increase in the Magnetic field causes a rise in the magnetic strength as well as the mass of the fluid particle so velocity decreases. Due to the effect of transverse magnetic field on electrically conducting fluid which gives rise to a resistive type of force called Lorentz force similar to drag force and increase in value of *M* leads to increase the drag force which slow down the motion of the fluid.

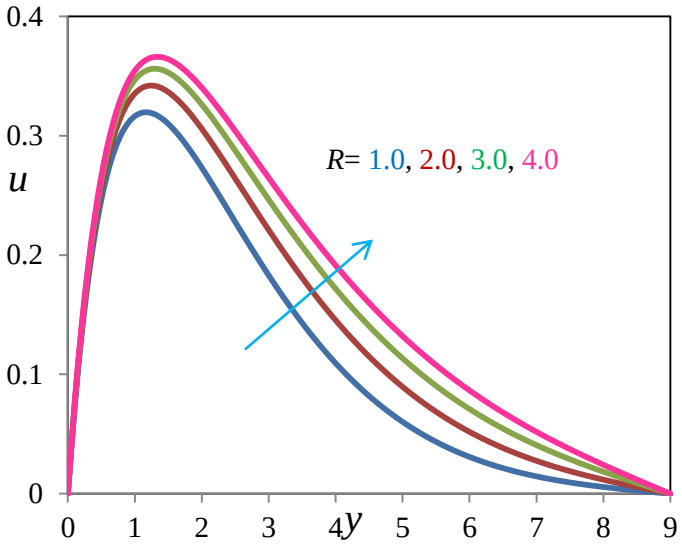

Figure 9. Velocity Profile for different values of *R* when *K=0.5, M=0.5, Ec=0.1, Sc=0.22, Gm=0.5, Pr=0.71, Gr=0.5,Kr=1.0*

Figures 9 and 10 illustrate the velocity and temperature profiles for different values of Radiation parameter *R*. Higher values of *R* imply higher surface heat flux and thereby making the fluid become warmer, this enhances the effect of the thermal buoyancy of the driving body force due to mass density variations which are coupled to the temperature and therefore, increasing the fluid velocity. The increase of Radiation parameter leads to increase of temperature profiles and to an increase of boundary layer thickness.

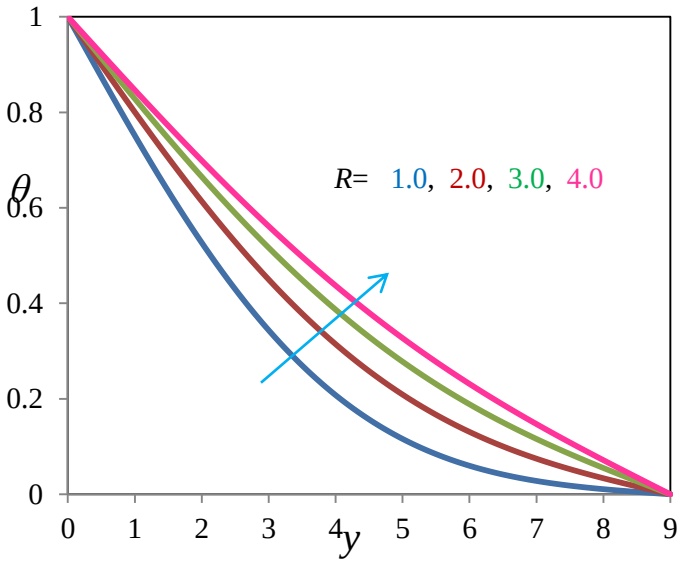

Figure 10. Temperature Profile for different values of *R* when *K=0.5, M=0.5, Ec=0.1, Sc=0.22, Gm=0.5, Pr=0.71, Gr=0.5, Kr=1.0*

Figures 11 and 12 illustrate the velocity and concentration profiles for different values of *Sc*. Schmidt number approximates the ratio of kinematic viscosity and mass diffusivity increasing of *Sc* leads to increasing in the viscous forces. When viscosity increase then internal resistance of the fluid will increase, so automatically the fluid velocity will decrease. The Schmidt number *Sc* embodies the ration of the momentum to the mass diffusivity. It quantifies the relative effectiveness of momentum and mass transport by diffusion in the hydrodynamic (velocity) & concentration (species) boundary layer. As *Sc* increases concentration decreases, this causes the concentration buoyancy effect to decrease yielding a reduction in the fluid velocity.

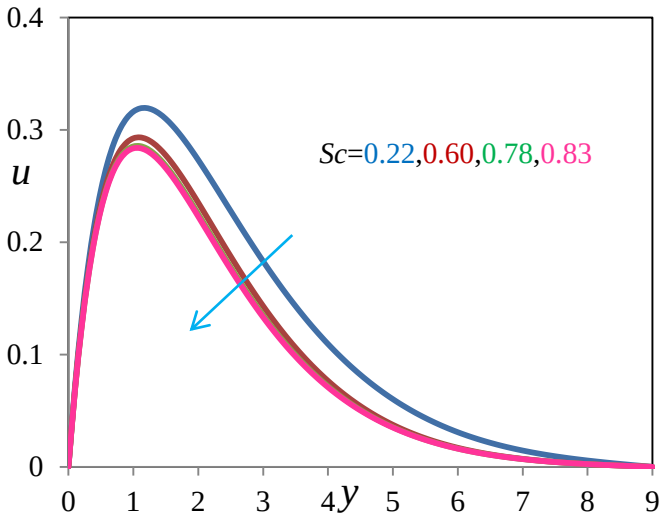

Figure 11. Velocity Profile for different values of *Sc* when *K=0.5, M=0.5, Ec=0.1, R=1, Gm=0.5, Pr=0.71, Gr=0.5, Kr=1.0*

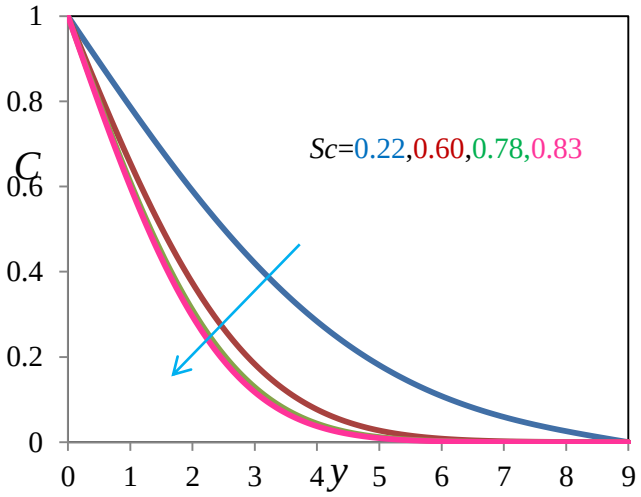

Figure 12. Concentration Profile for different values of Sc when *K=0.5, M=0.5, Ec=0.1, Pr=0.71 Gm=0.5, R=1.0, Gr=0.5, Kr=1.0*

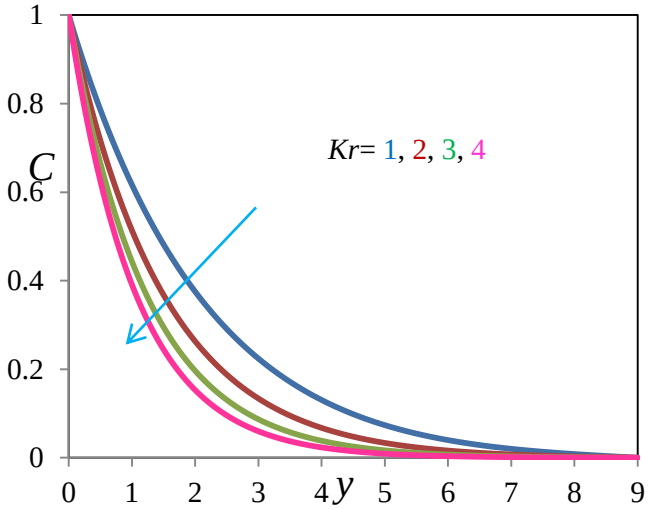

Figure 13. Concentration Profile for different values of *Kr* when *K=0.5, M=0.5, Ec=0.1, Pr=0.71 Gm=0.5, R=1.0, Gr=0.5, Sc=0.22*

The effects of the chemical reaction parameter *Kr* on the velocity, concentration profiles is shown in Figure 13. We noticed that an increase in the chemical reaction parameter leads to decrease in the concentration profile.

Table 2: skin friction (τ) coefficient for different values of parameters

Pr	*Sc*	*M*	*K*	*Gr*	*Ec*	τ	Prabhakar reddy et[3]
0.71	0.22	0.5	0.5	0.5	0.1	0.4598954	0.459896
7.00	0.22	0.5	0.5	0.5	0.1	0.2920192	0.292022
0.71	0.60	0.5	0.5	0.5	0.1	0.4261289	0.426130
0.71	0.22	1	0.5	0.5	0.1	0.4204118	0.420418
0.71	0.78	0.5	1	0.5	0.1	0.569358	0.569360
0.71	0.22	0.5	0.5	1	0.1	0.633764	0.633700
0.71	0.78	0.5	0.5	0.5	0.3	0.500913	0.500918

Table 3: Numerical data of Nusselt number (Nu) for different values of parameters

Pr	*Sc*	*M*	*K*	*Gr*	*Ec*	*Nu*	Prabhakar Reddy et[3]
0.71	0.22	0.5	0.5	0.5	0.1	0.3727429	0.372742
0.71	0.60	0.5	0.5	1.0	0.3	0.3718011	0.371802
0.71	0.22	1.0	0.5	0.5	0.5	0.3708576	0.370858

Table 4: Numerical data of Sherwood number (Sh) for different values of parameters.

Pr	*Sc*	*M*	*K*	*Gr*	*Sh*	Prabhakar et[3]
0.71	0.68	0.5	0.5	0.5	0.207853343	0.207852
1.00	0.22	1.0	0.5	0.5	0.343340231	0.343342
7.00	0.22	0.5	1.0	0.5	0.390978122	0.390970

Tables 2-4 shows the calculated values of skin friction, Nusselt number and Sherwood number for the present solution and are in good agreement with the published values of Prabhakar Reddy et [3]

CONCLUSION

In this paper we have studied the effects of thermal radiation on MHD Free convective flow of an incompressible fluid past a vertical plate in the presence of viscous dissipation. From present numerical study the following conclusions can be drawn

- The velocity increases with the increase of *Gr*, *Gm*, *Ec* and *K*
- The velocity and concentration decreases with an increase in Schmidt number.
- Increasing the prandtl number substantially decreases the velocity and the temperature profiles
- The velocity as well as temperature increases with an increase in the radiation parameter.
- Concentration decreases with an increase in chemical reaction parameter.

REFERENCES

1. Hossain MA, Mandal AC, Mass transfer effects on the unsteady hydromagnetic free convention flow past an accelerated vertical plate. J Phys D: Applied Phys 1985; 18:163-9.
2. Michalis Xenos, Stelios Dimas, Andreas Raptis, "MHD free convective flow of water near $4^{\circ}C$ past a vertical moving plate with constant suction", Applied Mathematics, 4 52-57, (2013).
3. B. Prabhakar Reddy, "Mass transfer effects on an unsteady MHD free convective flow of an incompressible viscous dissipative fluid past an infinite vertical porous plate", Int. J. of Applied Mechanics and Engineering, 2016 vol.21.No.1,pp 143-155.
4. Siva Reddy Sheri, R. Srinivasa Raju, "Soret effect on unsteady MHD free convective flow past a semi-infinite vertical plate in the presence viscous dissipation", International Journal for Computational Methods in Engineering Science and Mechanics**,** 16 (2) 132-141, (2015).
5. N. Pandya and A .K. Shukla International journal of mathematics and scientific computing (ISSN: 2231-5330) vol3, no 2, 2013.
6. A. Hussanan, M.Z. Salleh, R.M. Tahar, and I. Khan, PLoS ONE, 9, **(2014)**, DOI:10.1371/journal.pone.0108763.
7. Olarewaju PO. Similarity solution for natural convection from a moving vertical plate with internal heat generation and a convective boundary condition in the presence of thermal radiation and viscous dissipation. J Rep Opin 2012; 4(8):68–76.
8. H. A. Attia, and M. E. Sayed-Ahmed, Italian J. Pure and Appl. Math., 27, 19 **(**2010**).**
9. Venkateswarlu M, Ramna Reddy GV, Lakshmi DV. Effects of chemical reaction and heat generation on MHD boundary layer flow of a moving vertical plate with suction and dissipation. Int. J. Eng 2013; 1:27–38.
10. Sarada K, Shanker B. The effects of Soret and Dufour on an unsteady MHD free convection flow past a vertical porous plate in the presence of suction or injection. Int J Eng Sci 2013; 2:13–5.
11. N. Vedavathi, K. Ramakrishna and K. Jayarami Reddy, Radiation and mass transfer effects on unsteady MHD convective flow past an infinite vertical plate with Dufour and Soret effects, Ain Shams Engineering Journal, Volume 6, Issue 1, 363–371, 2015.
12. Ming-chun, LI., Yan-Wen, T., and Yu-Chun, Z. Soret and Dufour effects in strongly endothermic chemical reaction system of a porous medium. Trans. Nonferrous Met. Soc. China, 16, 1200-1204, 2006.
13. Srihari K, Srinivas Reddy G. Effects of Radiation and soret in the presence of heat source/sink on unsteady MHD flow past a semi-infinite vertical plate. Br J Math Comput Sci 2014; 4: 2536–56.
14. D. Srinivasacharya, Ch. RamReddy, Soret and Dufour effects on mixed convection from an exponentially stretching surface. Int. J. of Nonlinear Science, 12(1) (2011) 60-68, MCQ = 0.13 and AMS Math Sci Net Journal.
15. Rashidi MM, Vishnu Ganesh N, Abdul Hakeem AK, Ganga B. Buoyancy effect on MHD flow of Nanofluid over a stretching sheet in the presence of thermal radiation. J Mol Liq 2014;198: 234–8.
16. Srinivasa Rao G, Ramana B, Rami Reddy B, Vidyasagar G. Soret and Dufour effects on MHD boundary layer flow over a moving vertical porous plate with suction. Int J Emerg Trends Eng Dev 2014;2(4):215–26.
17. Mohammed Ibrahim S. Unsteady MHD convective heat and mass transfer past an infinite vertical plate embedded in a porous medium with radiation and chemical reaction under the influence of Dufour and Soret effects. Chem Process Eng Res 2014;19:25–38.
18. R. Srinivasa Raju, G. Jithender Reddy, J. Anand Rao, M.M. Rashidi and Rama Subba Reddy Gorla., (2016) Analytical and Numerical study of unsteady MHD free convection flow over an exponentially moving vertical plate with Heat Absorption, International Journal of Thermal Sciences, Volume 107, 303–315.
19. Yih K .A 1997 The effect of transpiration on coupled heat and mass transfer in mixed convection over a vertical plate embedded in a saturated porous medium.

International Communications in Heat and Mass transfer, 24(2) 265-275.

20. G.V. Ramana reddy , Ch .V. Ramana Murthy and N. Bhasker reddy Unsteady MHD free convective Mass transfer flow past an infinite vertical porous plate with variable suction and soret effect.
21. J.Anand Rao, P. Ramesh Babu and R. Srinivasa Raju, Finite element analysis of unsteady MHD free convection flow past an infinite vertical plate with Soret, Dufour thermal radiation and heat source.
    ARPN Journal of Engineering and Applied sciences. Volume 10, No 12, 2015.
22. G D Smith. Numerical solution of Partial Differential Equations, Oxford University Press London
23. An Introduction to the Finite element method, Third edition by J.N Reddy (Tata McGraw-Hill)